

Development of a Real-Time Aeroperformance Analysis Technique for the X-29A Advanced Technical Demonstrator

Ronald J. Ray* and John W. Hicks*
NASA Ames Research Center, Edwards, California
and

Russ I. Alexander†
Computing Devices Company, Ottawa, Canada

The X-29A advanced technology demonstrator has shown the practicality and advantages of the capability to compute and display, in real-time, aeroperformance flight results. This capability includes the calculation of the in-flight measured drag polar, lift curve, and aircraft specific excess power. From these elements, many other types of aeroperformance measurements can be computed and analyzed. The technique can be used to give an immediate postmaneuver assessment of data quality and maneuver technique, thus, increasing the productivity of a flight program. A key element of this new method was the concurrent development of a real-time, in-flight, net-thrust algorithm, based on the simplified gross thrust method. This net-thrust algorithm allows for the direct calculation of total aircraft drag.

Nomenclature

| | |
|------------|---|
| A | = area, ft ² |
| C_D | = coefficient of drag |
| C_L | = coefficient of lift |
| D | = aircraft drag, lb |
| F_{ex} | = excess thrust, lb |
| F_G | = gross thrust, lb |
| F_N | = engine net-thrust available, lb |
| F_{NP} | = net propulsive force, lb |
| F_R | = ram drag, lb |
| FVG | = fan variable guide vanes |
| HPVG | = high-pressure compressor variable guide vanes |
| L | = aircraft lift, lb |
| M | = Mach number |
| $N1$ | = fan rotor speed, rpm |
| $N2$ | = compressor rotor speed, rpm |
| n_x | = aircraft longitudinal acceleration, g |
| n_y | = aircraft lateral acceleration, g |
| n_z | = aircraft normal acceleration, g |
| P | = pressure, lb/in. ² |
| P_s | = specific excess power, ft/s |
| \dot{p} | = roll rate, deg/s |
| \ddot{p} | = roll acceleration rate, deg/s ² |
| \bar{q} | = dynamic pressure, lb/in. ² |
| \dot{q} | = pitch rate, deg/s |
| \ddot{q} | = pitch acceleration, deg/s ² |
| \dot{r} | = yaw rate, deg/s |
| \ddot{r} | = yaw acceleration rate, deg/s ² |
| S | = reference wing area, ft ² |
| T | = temperature, °C |

| | |
|-----------|-----------------------------|
| V_t | = true airspeed, ft/s |
| \dot{W} | = mass flow rate, lb/s |
| Wt | = aircraft gross weight, lb |
| α | = angle of attack, deg |
| σ | = standard deviation, % |
| β | = angle of sideslip, deg |

Subscripts

| | |
|------|-------------------------------|
| AB | = afterburner |
| AP | = area-pressure thrust method |
| $B3$ | = engine compressor bleed air |
| b | = body axis |
| F | = fuel |
| i | = indicated |
| P | = primary |
| S | = static |
| T | = total |
| WT | = mass-flow thrust method |
| w | = wind axis |

Engine Stations

| | |
|-----|---------------------------|
| 0 | = freestream |
| 1 | = engine inlet |
| 3 | = compressor exit |
| 5 | = turbine rotor discharge |
| 558 | = turbine exhaust exit |
| 6 | = afterburner inlet |
| 7 | = exhaust nozzle inlet |
| 8 | = exhaust nozzle throat |
| 9 | = exhaust nozzle exit |

Introduction

AIRCRAFT performance flight-test data have traditionally been calculated and analyzed after the test flight has ended. This postflight analysis often has revealed errors and other inadequacies in the data that were serious enough to require that the flight test be repeated. The capability to calculate and display performance data for ground monitoring while a flight was still in progress would significantly improve

Received Aug. 3, 1989; revision received Jan. 12, 1990. Copyright © 1990 by the American Institute of Aeronautics and Astronautics, Inc. No copyright is asserted in the United States under Title 17, U.S. Code. The U.S. Government has a royalty-free license to exercise all rights under the copyright claimed herein for Governmental purposes. All other rights are reserved by the copyright owner.

*Aerospace Engineer, Dryden Flight Research Center.

†Aerospace Engineer.

flight productivity by allowing rapid and accurate real-time evaluation of flight-test maneuver techniques and data quality. If the data from a maneuver were judged to be unacceptable, the maneuver could be repeated immediately while flight-test conditions were suitable.

Because of the limited test time available during the X-29A flight-test program to define the performance potential of the forward-swept wing and its related technologies, the need for a real-time performance data analysis capability was especially critical. This real-time capability, coupled with dynamic flight maneuver techniques, would also provide a way to assess maneuver dynamic effects and instrumentation system malfunctions. Safety of flight monitoring capability would also be improved. Previous efforts have proven the benefits of real-time analysis techniques.¹

This paper describes a real-time aeroperformance analysis capability developed at the NASA Ames-Dryden Flight Research Facility to calculate and display in graphical form aerodynamic data such as drag polars and lift curves along with engine performance parameters. Integral to this capability was the development of a real-time, in-flight, net-thrust algorithm based on the simplified gross thrust method (SGTM) of the Computing Devices Company (ComDev) of Ottawa, Canada.²

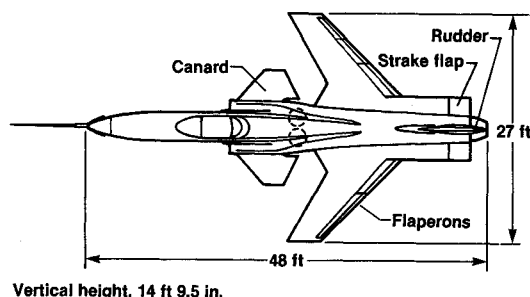


Fig. 1 The X-29A advanced technology demonstrator.

This new technique was developed under a joint agreement between the United States and Canada using data obtained during the thrust calibration test of the X-29A performance engine at the NASA Lewis Research Center's Propulsion System Laboratory (PSL).³ Typical flight results are presented along with an assessment of the in-flight uncertainty of the real-time, net-thrust method.

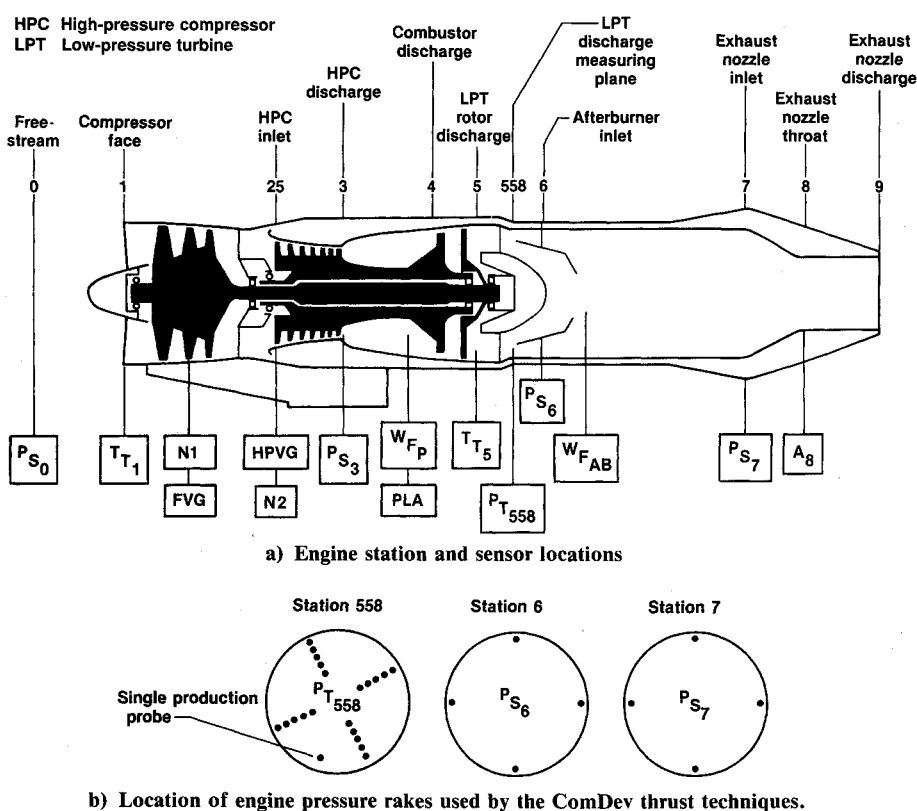
Aircraft Description

The X-29A (see Fig. 1) is a single-seat, fighter-type aircraft incorporating several new technology concepts that integrally work together for aircraft performance improvements. The most notable feature is the forward-swept wing with a 29.3-deg, leading-edge sweep and a 5% thin supercritical airfoil section. The upper and lower surface wing skins are made of a graphite-epoxy composite material and are aeroelastically tailored to inhibit wing structural divergence. The wing has no leading-edge devices but incorporates full-span trailing-edge, dual-hinged flaperons that are divided into three segments on each wing. Wing camber is automatically controlled by the flight control system. The aircraft's 35% negative static margin requires a high level of stability augmentation, which is provided by a triply redundant digital fly-by-wire flight control system with an analog backup.

The aircraft is powered by a single 16,000-lb class General Electric F404-GE-400 afterburning engine. The engine is mounted in the fuselage with two side-mounted, fixed geometry inlets. Maximum aircraft takeoff gross weight is 17,800 lb with a 4000-lb fuel capacity.

Data Acquisition System

The X-29A onboard data acquisition system uses both pulse code modulation (PCM) and frequency modulation (FM) for data encoding. The 10-bit PCM system samples data from 25 to 400 samples/s depending on the desired frequency range to be covered. A total of 691 measured data parameters was telemetered to the ground for recording, real-time analysis, and control room monitoring. The data parameter set included



b) Location of engine pressure rakes used by the ComDev thrust techniques.

Fig. 2 Engine instrumentation system

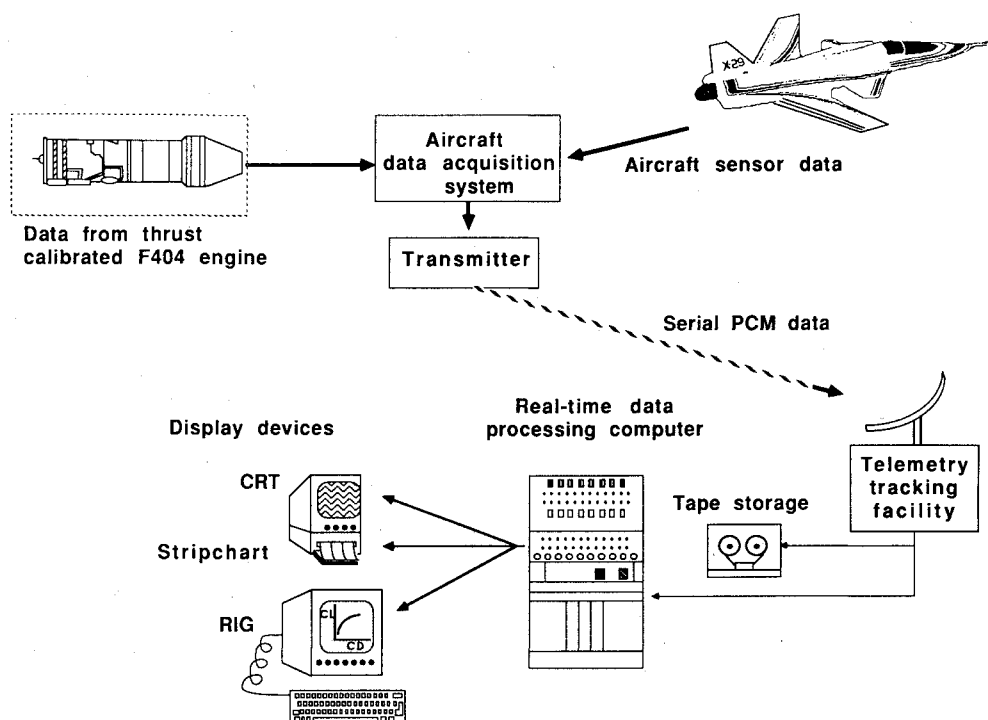


Fig. 3 The X-29A real-time performance data system.

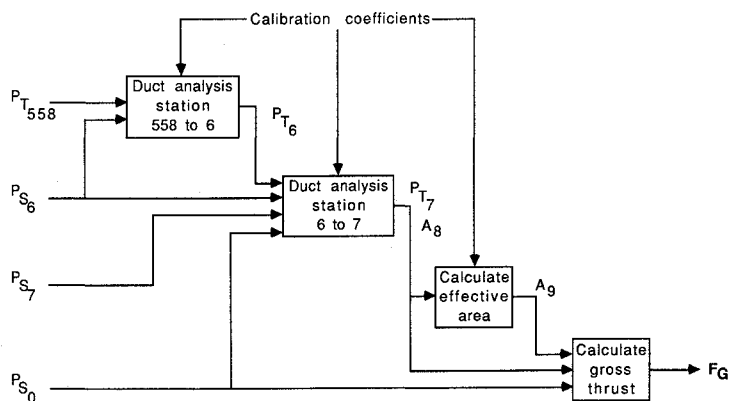


Fig. 4 Flowchart of the SGTM.

measurements for structural loads, structural dynamics, flight controls, stability and control, aircraft subsystems, propulsion and performance, wing deflections, buffet, and external pressure distributions.

Aircraft instrumentation included a pitot-static noseboom with angle of attack (α) and sideslip angle (β) vanes. The instrumentation package used for the flight performance measurements included two body-mounted linear accelerometer packages and a rate gyro package for aircraft pitch, roll, and yaw attitudes, rates, and angular accelerations.

The F404-GE-400 engine has a complete instrumentation system for monitoring engine operating characteristics, engine trim levels, and for calculating in-flight thrust. Measurement locations are shown in Fig. 2 and included inlet total temperature (T_{T_i}), fan and compressor rotor speeds ($N1$ and $N2$), combustor static pressure (P_{S_3}), turbine exhaust temperature (T_{T_5}), nozzle throat area (A_8), and a 20-probe rake measurement of turbine exhaust pressure ($P_{T_{558}}$). Volumetric flow meters were used to measure main engine fuel flow (W_{F_p}) and afterburner pilot and main fuel flows ($W_{F_{AB}}$).

In order to implement the real-time, in-flight thrust method discussed in this paper, four flush-mounted static pressure taps

were located at both the afterburner entrance (P_{S_6}) and exhaust nozzle entrance (P_{S_7}). This technique also made use of the engine $P_{T_{558}}$ rake, T_{T_5} , freestream static air pressure (P_{S_0}), and true airspeed (V_t).

Real-Time Data Processing and Display

The X-29A real-time performance data system is designed to record data from the aircraft data acquisition system, then to process and display the information in the mission control room. An illustration of this system is shown in Fig. 3. Data from the aircraft is transmitted in a serial data stream and received by the telemetry tracking facility on the ground. The data stream is then passed along land lines to a mission control center for data storage, processing, and display. These facilities make up part of the NASA Dryden Western Aeronautical Test Range.⁴

For security reasons, X-29A flight data are telemetered in an encrypted format. The serial data are decrypted, synchronized, and demultiplexed in the mission control center. An analog tape recorder is used to store this raw aircraft data for postflight processing. The raw data are also passed to a Gould

The RIG system stores a number of predefined display formats that can be selected by the operator as required. Graphic parameters are updated at up to 10 samples/s, and the column of digital data displayed next to the graphics is updated at 1 sample/s. The actual calculation rate of the performance parameters is up to 12.5 samples/s. The RIG operator not only controls which graphic page (format) to display but also can start, stop, clear, and print the display at any time. The RIG system has been upgraded with a new system capable of creat-

The SGTm computes gross thrust based on a one-dimensional analysis of the flow in the engine afterburner and exhaust nozzle. Figure 4 shows a block diagram of the algorithm. The algorithm analyzes the flow in the afterburner duct from the turbine exit (station 558) to the exhaust nozzle exit (station 9) and determines first the total pressure at the afterburner entrance (P_{T_6}) and then at the exhaust nozzle entrance (P_{T_7}). The exhaust nozzle throat area (A_8) is also computed. Gross thrust is then computed from the calculated value of P_{T_7} and

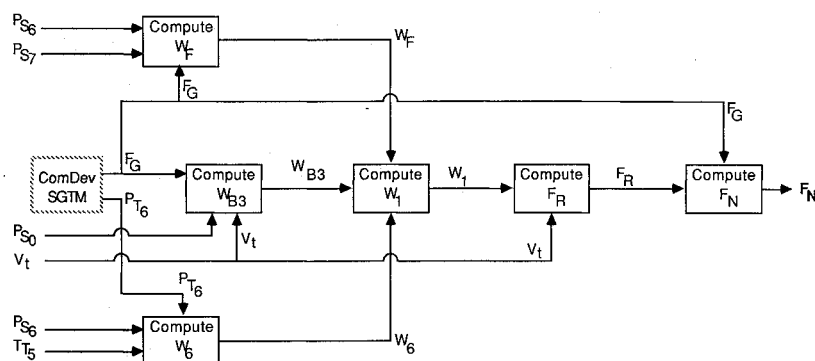


Fig. 5 Flowchart of the SNTM.

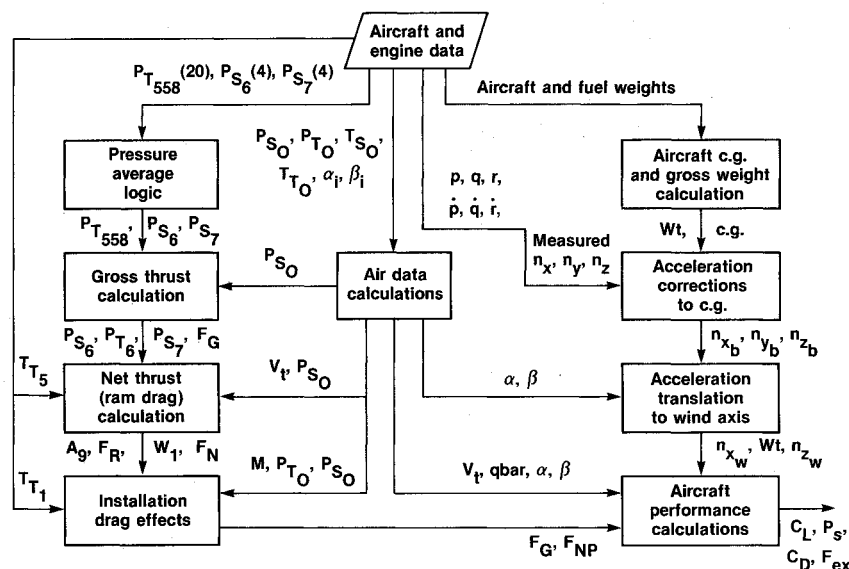


Fig. 6 The X-29A real-time performance calculation flowchart.

A_8 and measured nozzle static pressure. The SGTm also computes exhaust nozzle exit area (A_9) by applying computed A_8 and the mechanical A_9/A_8 schedule.

Calibration coefficients for the F404 engine were determined using data obtained during testing at the Lewis PSL Facility. Pressure and thrust data were collected from 131 data points at 11 combinations of Mach number and altitude over the range of engine power settings from near flight idle to maximum afterburning. The coefficients were applied to the equations to correct for the effects of internal friction, mass transfer (leakages), three-dimensional effects, and the effect of the simplifying assumptions used in the theory. Calibration coefficients obtained through calibration of the individual engine provide good accuracy for all engines of the same model.

More recently, ComDev has developed an accurate and fast net-thrust algorithm for the F404 engine. A block diagram of the simplified net thrust method (SNTM) is shown in Fig. 5. The SNTM uses the same P_{S_6} and P_{S_7} pressure measurements as the SGTm and also uses the production T_{T_5} measurement and calculated true velocity (V_t).

Net thrust (F_N) is defined as gross thrust (F_G) minus inlet airflow momentum or ram drag (F_R).

$$F_N = F_G - F_R$$

Ram drag is defined as the product of V_t and mass flow rate (W_1).

$$F_R = V_t W_1 / g$$

The ComDev SGTm calculates F_G , P_{T_6} , and A_9 . The SNTM calculates W_1 and obtains V_t from the aircraft airdata system to determine ram drag and thus net thrust.

Inlet mass flow is determined by calculating mass flow rate at the afterburner entrance (station 6), using flow parameters determined in the SGTm gross thrust algorithm and the turbine discharge total temperature measured by existing engine instrumentation. This mass flow rate (W_6) is used to compute the inlet mass flow rate after accounting for compressor bleed air extraction (W_{B3}) and fuel mass addition (W_F) using an empirical model calibrated with test data from the Lewis PSL facility. The inlet mass flow is thus computed by

$$W_1 = W_6 - W_F + W_{B3}$$

The SNTM calculates engine station 6 local Mach number (M_6) and mass flow rate (W_6) using measured T_{T_5} and P_{S_6} and calculated P_{T_6} . Total temperature at station 6 (T_{T_6}) is assumed to equal T_{T_5} . A simplified main engine fuel flow (W_F), in comparison to calculated inlet airflow relationship, was derived empirically from Lewis PSL facility data.

A constant bleed air extraction (W_{B3}) was assumed based on aircraft system cooling air requirements. Over the aircraft operating envelope, the flows W_F and W_{B3} are much smaller than W_6 (typically less than 2% of W_6). Therefore, errors in their determination have only secondary effects on W_1 accuracy. The accuracy of the production engine mounted T_{T_5} measuring system is adequate because the sensitivity of computed net thrust to T_{T_5} errors is small. A 10°F error in T_{T_5} , for example, produces an error of only 0.03% in net thrust at intermediate rated power (IRP) at Mach 0.9, 30,000 ft.

The SNTM was also calibrated using Lewis PSL data. Because the mass flow is calculated in the engine afterburner section, where the gas flow is well mixed, inlet flow distortion effects are minimized.

Data Analysis Method

The drag polar analysis technique was based on the accelerometer method. The measured body-axis accelerometer data were corrected for angular rate and center of gravity (c.g.)

position then transformed to the aircraft wind axis of flight path system by angular transformations through α and β . Thrust installation corrections included estimated nozzle drag (D_{NOZ}) and spillage drag (D_{SPIL}).

Aircraft coefficients of lift (C_L) and drag (C_D) were computed from the accelerometer method⁸ using equations

$$C_D = \frac{D}{\bar{q}S} = \frac{F_{NP} - F_{ex}}{\bar{q}S}$$

$$C_L = \frac{L}{\bar{q}S} = \frac{n_z W_t - F_G \sin \alpha}{\bar{q}S}$$

where

$$F_{ex} = n_x W_t$$

$$F_{NP} = F_N - (D_{SPIL} + D_{NOZ})$$

Aircraft P_s was computed from the accelerometer data as follows

$$P_s = F_{ex} V_t / W_t$$

The input data to the real-time performance program were not filtered (except for an onboard, antialiasing filter for acceleration parameters), nor were trim drag corrections applied to the drag results. The real-time display values were neither smoothed nor thinned (below the 10 samples/s update rate of the RIG system), and wild points were neither edited nor removed. This allowed the fastest calculation rate possible in real time and the ability to evaluate data quality without the extra data massaging. The time lag between the actual flight event and the display of calculated performance data on the RIG is estimated to be under 0.25 s.

Real-time software was developed to implement the aircraft and engine performance analysis techniques. Figure 6 summarizes the performance calculations in a flow diagram. The X-29A air data software was used to obtain α and β and Mach number (M). Indicated angle of attack (α_i) was corrected for upwash errors, misalignment errors, pitch-rate effects, boom bending, and fuselage bending effects. Mach number was computed from nose-boom pitot static measurements. A pressure averaging routine was also developed to process engine pressure rake data.

Maneuver Techniques

Dynamic flight-test techniques were used to define quickly and accurately the aircraft drag polar and lift curve characteristics at a given Mach number over a wide range of α . These

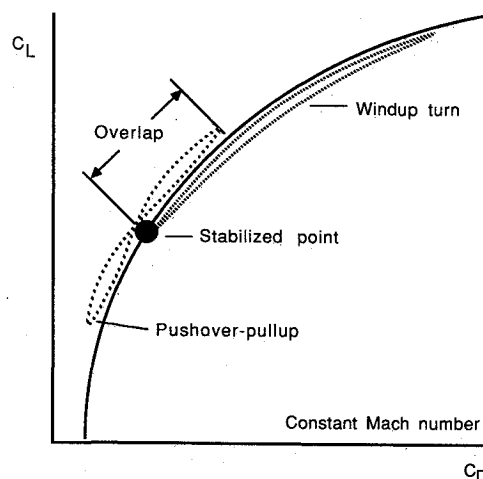


Fig. 7 Schematic of maneuvers to define a drag polar.

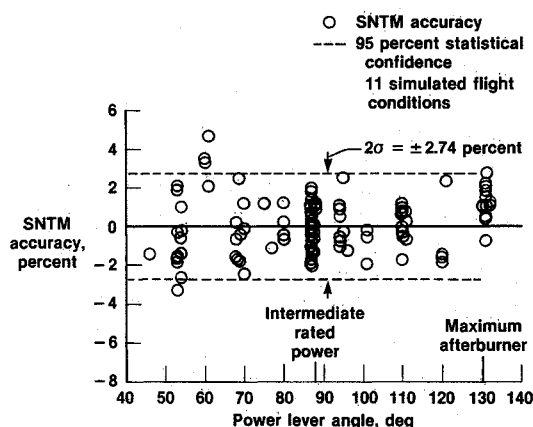


Fig. 8 Accuracy of the SNTM determined at Lewis PSL facility.

Table 1 Estimated in-flight uncertainty of the ComDev simplified gross and net thrust methods

| Mach | Altitude, ft | PLA, deg | Uncertainty | |
|------|--------------|----------|-------------|---------|
| | | | SGTM, % | SNTM, % |
| 0.4 | 10,000 | 70 | 2.35 | 3.61 |
| | | 87 | 1.36 | 2.41 |
| | | 130 | 0.99 | 2.10 |
| 0.8 | 10,000 | 70 | 2.52 | 3.61 |
| | | 87 | 1.32 | 2.41 |
| | | 130 | 1.06 | 2.10 |
| 0.9 | 30,000 | 70 | 2.61 | 4.25 |
| | | 87 | 1.48 | 3.15 |
| | | 130 | 1.05 | 2.75 |
| 1.2 | 30,000 | 70 | 1.28 | 2.69 |
| | | 87 | 1.36 | 2.69 |
| | | 130 | 1.04 | 2.72 |
| 0.8 | 40,000 | 70 | 2.55 | 3.65 |
| | | 87 | 1.82 | 4.39 |
| | | 130 | 1.09 | 2.86 |
| 1.6 | 40,000 | 70 | 1.36 | 2.81 |
| | | 87 | 1.36 | 2.81 |
| | | 130 | 1.04 | 2.74 |

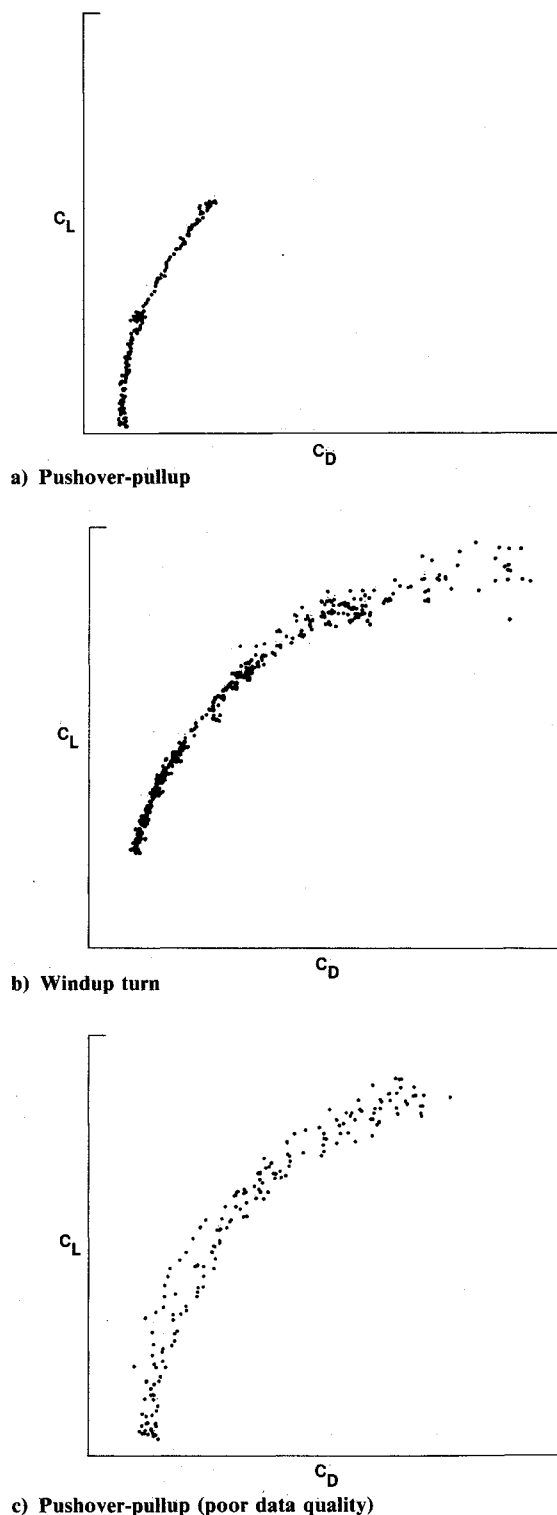
maneuver techniques rely on accelerometer methods using body-mounted accelerometer packages to measure aircraft accelerations along and normal to the flight path.

Two dynamic maneuvers, the pushover-pullup and the windup turn, were manually flown on the X-29A to define complete drag polar curves. Both maneuvers were preceded by 30-s stabilized trim points. The pushover-pullup was used to obtain the mid- to low-range of α . The maneuver test technique consisted of a pushover from the 1-g normal load factor (n_z) at the stabilized flight condition to 0 g at a nominal g-onset rate of -0.2 g/s . At the 0-g point, the aircraft was pulled up at a 0.2 g/s onset rate to 2 g and then returned to the 1-g level flight condition. Altitude and Mach number excursions were kept to a minimum, while power lever angle (PLA) was held constant. The windup turn maneuver was used to obtain data from the mid-range to high-range of α . Using the same g-onset rate as for the pushover-pullup maneuver, the windup turn was flown at a fixed power setting with the aircraft descending, trading altitude for airspeed in order to hold a constant Mach number as the normal load factor and α were increased to the aim conditions. For a given Mach number, the maneuvers produced flight data that overlapped in coefficient of lift between 1 and 2 g giving a full polar shape over α and assuring good data correlation between the maneuvers. Figure 7 gives a schematic drag polar representation of the maneuvers' sweep of the α variation of a polar at a constant Mach number. Further discussions of the X-29A flight-test techniques can be found in Ref. 9.

Results and Discussion

Net Thrust Uncertainty

An analysis was conducted to determine the accuracy of the real-time performance values as affected by the net-thrust calculation. The net-thrust values calculated by the SNTM method were compared to measured values obtained in the Lewis PSL facility. The percent error in SNTM, expressed as a percentage of measured net thrust, is plotted against PLA in Fig. 8. The bias error, over the 131 test points at 11 simulated flight conditions, was 0% and the 95% statistical confidence limit (two standard deviations, 2σ) was $\pm 2.74\%$. This spread



c) Pushover-pullup (poor data quality)

Fig. 9 Examples of real-time aircraft performance data.

includes contributions from all the input measurement errors and the SNTM net thrust model error determined from Lewis PSL data.

A sensitivity analysis was conducted to determine the expected in-flight uncertainty of the SNTM. Net-thrust uncertainty was calculated by combining the model error and the individual errors due to the error in each input measurement by the method of root-sum squares. Table 1 shows the in-flight total uncertainties of SNTM net thrust for six Mach number and altitude conditions at three power settings. The uncertainty at IRP (PLA = 87 deg) ranges from $\pm 2.41\%$ at Mach 0.8, 10,000 ft to $\pm 4.39\%$ at Mach 0.8, 40,000 ft. At Mach 0.9, 30,000 ft design point, the total uncertainty of the SNTM at IRP is $\pm 3.15\%$, and, at maximum afterburning, it is $\pm 2.75\%$.

These results verify that highly accurate net-thrust values have been calculated in real time on the X-29A aircraft. The sensitivity of calculated lift and drag due to independent parameters such as thrust and α was evaluated for the X-29A in Ref. 10. Based on these results, the uncertainty in the real-time C_D value due to the uncertainty in net thrust is estimated to be about $\pm 3.0\%$. The effects of α uncertainty on C_L and C_D can also be substantial.

Flight Results

The use of real-time performance calculations allowed an immediate assessment of data quality and maneuver technique. Figure 9 shows typical drag polars obtained during various performance maneuvers. The pushover-pullup maneuver (see Fig. 9a) sweeps out the lower α portion of the drag polar, whereas the windup turn maneuver (see Fig. 9b) overlaps and completes the higher α section of the curve as discussed in the Maneuver Techniques section of this paper. These results illustrate the data quality obtained in real time during X-29A performance testing. A maneuver that misses the aim flight conditions can be terminated and repeated immediately, greatly increasing productivity and reducing the postflight data processing requirements.

Figure 9c shows an example of a poor quality pushover-pullup maneuver, which is evident by the increased data scatter compared to Fig. 9a. This data scatter resulted, in part, due to

improper aerodynamic surface positions caused by maneuver dynamics.¹¹ This scatter can occur when the flight control inputs are too abrupt for the flaperons, strake flaps, or canard to follow optimum schedules. Other factors that may affect the performance maneuver quality include buffet, off Mach or altitude conditions, and pilot technique.¹²

The ability to monitor performance data quality and the function of the instrumentation system in real time proved a very effective diagnostic capability. During the initial checkout of the thrust instrumentation system, the engine pressure averaging logic helped to detect and isolate pressure leaks and transducer failures. The ComDev real-time thrust algorithms also helped in the flight safety monitoring of the X-29A engine performance during takeoff checks and flight.

To evaluate the in-flight calculation of thrust using the SNTM, comparisons were made to the thrust values calculated by the engine manufacturer's in-flight thrust program. This postflight program computes net thrust by two methods: the area-pressure method (F_{NAP}) and the mass flow method (F_{NWT}).¹³ These two methods were also calibrated using Lewis PSL data.

The three net-thrust methods were compared during post-flight processing of over 150 performance maneuvers including windup turns, pushover-pullups, level accelerations and decelerations, stabilized level flight, and takeoff. Figure 10 shows some typical results. The three net thrust methods agreed within their expected in-flight uncertainties. For example, Fig. 10a shows flight data from a sustained high-g turn at maximum power at Mach 0.9 and 30,000 ft. Net thrust computed by the SNTM and in-flight thrust program fall within a band of $\pm 2.7\%$ throughout the maneuver. The thrust increase shown in this figure is due to decreasing altitude and increasing Mach during the maneuver. Flight conditions shown in this figure are target conditions. Figure 10b shows a comparison of the three thrust methods shortly following an IRP takeoff. The net-thrust values show little change during the maneuver because the aircraft is both climbing and accelerating causing a cancellation effect. Postflight comparisons show the SNTM typically falls between the F_{NAP} and F_{NWT} values as shown in Fig. 10b. These results give confidence to the predicted accuracies of the SNTM presented in this paper.

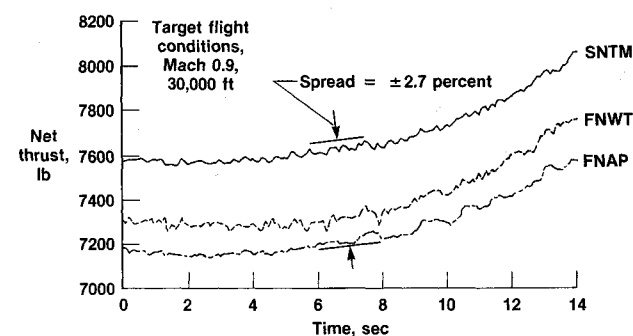
Concluding Remarks

The practicality and advantages of a real-time performance analysis technique were demonstrated during flight testing of the X-29A. This technique has enhanced the flight productivity and efficiency of the flight research program. It also helped to assess data quality, instrumentation functionality, and maneuver technique. A key element in the success of the real-time performance technique was the development of the Computing Devices Company's simplified net-thrust method. This net-thrust algorithm allows for the rapid calculation of aircraft thrust and drag and enhanced the safety of flight monitoring of the propulsion system. Because accurate net-thrust values were calculated by the SNTM, the uncertainties in real-time C_D results due to the uncertainty in net thrust were estimated to be about $\pm 3\%$.

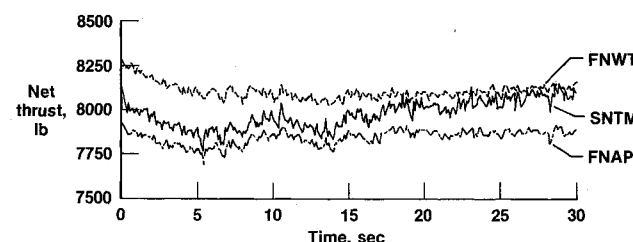
The real-time performance analysis provides a major advancement in flight-test productivity and efficiency by increasing aircraft diagnostic capabilities related to aircraft performance flight testing resulting in decreased downtime and postflight data requirements. Results show good agreement with uncertainty predictions and compare favorably to post-flight techniques.

References

- Hicks, J. W., and Peterson, K. L., "Real-Time Flight Analysis and Display Techniques for the X-29A Aircraft," AGARD CP-452, Oct. 1988.
- Kurtenbach, F. J., "Evaluation of a Simplified Gross Thrust Cal-



a) Windup turn, maximum power, 0.9 Mach, 30,000 ft.



b) IRP takeoff, Edwards Air Force Base

Fig. 10 Comparison of in-flight net thrust calculated by three methods.

ulation Technique Using Two Prototype F100 Turbofan Engines in an Altitude Facility," NASA TP-1482, June 1979.

³Burns, M. E., and Kirchgesner, T. A., "Airflow Calibration and Exhaust Pressure Temperature Survey of an F-404, S/N 215-209, Turbofan Engine," NASA TM-100159, Sept. 1987.

⁴Moore, A. L., "The Western Aeronautical Test Range of NASA Ames Research Center," NASA TM-85924, Jan. 1985.

⁵Malone, J. C., and Moore, A. L., "Western Aeronautical Test Range Real-Time Graphics Software Package MAGIC," NASA TM-100425, May 1988.

⁶Baer-Riedhart, J. I., "Evaluation of a Simplified Gross Thrust Calculation Method for a J85-21 Afterburning Turbojet Engine in an Altitude Facility," AIAA Paper 82-1044, June 1982.

⁷Kurtenbach, F. J., and Burcham, F. W., Jr., "Flight Evaluation of a Simplified Gross Thrust Calculation Technique Using an F100 Turbofan Engine in an F-15 Airplane," NASA TP-1782, Jan. 1981.

⁸Hicks, J. W., and Huckabone, T., "Preliminary Flight-Deter-

mined Subsonic Lift and Drag Characteristics of the X-29A Forward-Swept-Wing Airplane," NASA TM-100409, Aug. 1989.

⁹Hicks, J. W., Cooper, J. M., Jr., and Sefic, W. J., "Flight Test Techniques for the X-29A Aircraft," AIAA Paper 87-0082, Jan. 1987.

¹⁰Powers, S. G., "Predicted X-29A Lift and Drag Coefficient Uncertainties Caused by Errors in Selected Parameters," NASA TM-86747, Oct. 1985.

¹¹Hicks, J. W., and Moulton, B. J., "Effects of Maneuver Dynamics on Drag Polars for an Aircraft With Automatic Wing Camber Control," AIAA Paper 88-2144, May 1988.

¹²Hicks, J. W., Kania, J., Pearce, R., and Mills, G., "Challenges in Modeling the X-29A Flight Test Performance," AIAA Paper 87-0081, Jan. 1987.

¹³Burcham, F. W., Jr., "An Investigation of Two Variations of the Gas Generator Method to Calculate the Thrust of the Afterburning Turbofan Engines Installed in an F-111A Airplane," NASA TN D-6297, April 1971.

Attention Journal Authors: Send Us Your Manuscript Disk

AIAA now has equipment that can convert **virtually any disk** (3½-, 5¼-, or 8-inch) **directly to type**, thus avoiding rekeyboarding and subsequent introduction of errors.

You can help us in the following way. If your manuscript was prepared with a word-processing program, please *retain the disk* until the review process has been completed and final revisions have been incorporated in your paper. Then send the Associate Editor *all* of the following:

- Your final version of double-spaced hard copy.
- Original artwork.
- A *copy* of the revised disk (with software identified).

Retain the original disk.

If your revised paper is accepted for publication, the Associate Editor will send the entire package just described to the AIAA Editorial Department for copy editing and typesetting.

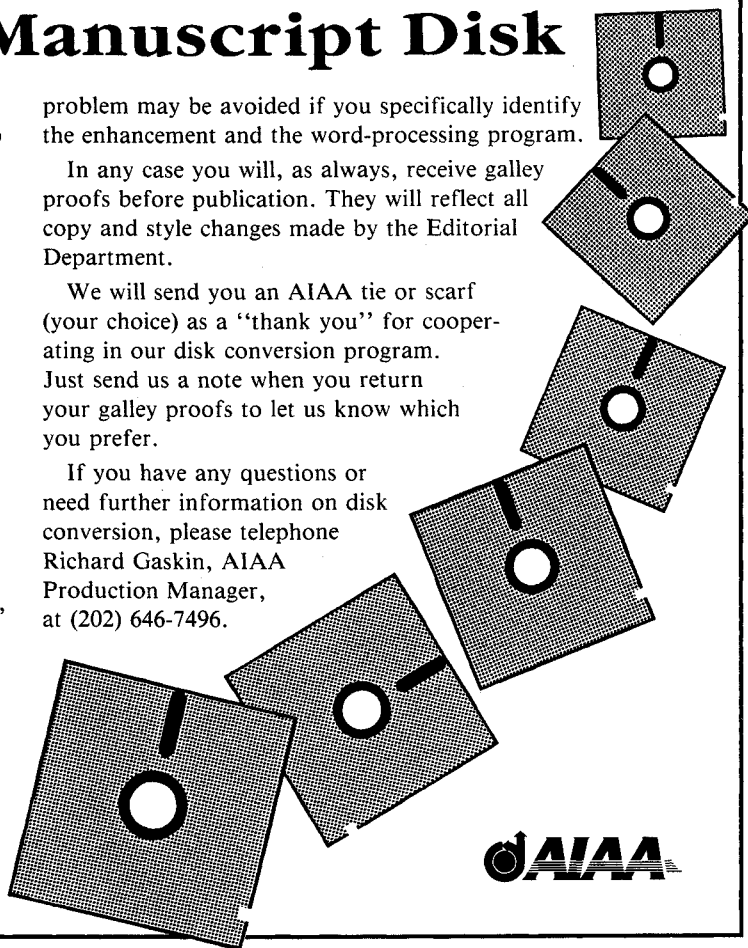
Please note that your paper may be typeset in the traditional manner if problems arise during the conversion. A problem may be caused, for instance, by using a "program within a program" (e.g., special mathematical enhancements to word-processing programs). That potential

problem may be avoided if you specifically identify the enhancement and the word-processing program.

In any case you will, as always, receive galley proofs before publication. They will reflect all copy and style changes made by the Editorial Department.

We will send you an AIAA tie or scarf (your choice) as a "thank you" for cooperating in our disk conversion program. Just send us a note when you return your galley proofs to let us know which you prefer.

If you have any questions or need further information on disk conversion, please telephone Richard Gaskin, AIAA Production Manager, at (202) 646-7496.



AIAA